Available online at www.sciencedirect.com
ScienceDirect
Journal of African Earth Sciences 48 (2007) 341–352
Journal of African Earth Sciences
www.elsevier.com/locate/jafrearsci

Plio-Pleistocene microtephra in DSDP site 231, Gulf of Aden

Sarah J. Feakins [a,*], Francis H. Brown [b], Peter B. deMenocal [a]

[a] Lamont-Doherty Earth Observatory, P.O. Box 1000, NY 10964, United States
[b] University of Utah, Salt Lake City, Utah 84112-0011, United States

Received 13 November 2006; received in revised form 5 April 2007; accepted 8 May 2007
Available online 24 May 2007

Abstract

We reconstruct a Plio-Pleistocene microscopic tephrostratigraphy for DSDP Site 231 in the Gulf of Aden. Systematic microtephrostratigraphy increases the potential for identifying tephra horizons for regional stratigraphic correlation and age control, as well as providing information about eruptive histories. Microtephra reveal three main pulses of volcanism c. 4.0–3.2 Ma, 2.4 Ma and 1.7–1.3 Ma, corresponding to peaks in volcanic activity recorded in the East African Rift System. Previous studies of DSDP Site 231 have reported six visible tephra horizons (up to 25 cm thick) with geochemical compositions matching East African tuffs. We find 68 additional microtephra horizons through microscopic examination of 1050 samples (each integrating c. 3 ka) in over 200 m of marine sediments. We report the major and minor element geochemical compositions of individual glass shards in six of these microtephra horizons and establish a robust correlation at 168.73 m to the Lokochot Tuff (3.58 Ma), which together with previously identified tephra, provides a tightly constrained chronostratigraphy for the mid Pliocene.

Keywords: Tephra; Microtephra; Cryptotephra; Volcanic glass; Electron microprobe; East Africa; Gulf of Aden; Lokochot

1. Introduction

Volcanic activity associated with late Neogene rifting and uplift has provided a tephrostratigraphic framework with which to date and correlate sedimentary sequences in and around East Africa, including the fossil record of hominin evolution (e.g., Brown and Feibel, 1986; Walter and Aronson, 1993; Clark et al., 1994; WoldeGabriel et al., 2005; Brown et al., 2006). Where tephra glass shards can be correlated geochemically between depositional archives, they provide a time-equivalent stratigraphic horizon, independent of dating uncertainties. Tephra ejected from explosive volcanic eruptions in the Afro-Arabian rift have been found in marine sediments at up to 2700 km from source volcanoes (Sarna-Wojcicki et al., 1985; Brown et al., 1992; deMenocal and Brown, 1999; Peate et al., 2003), providing age control for marine paleoclimate records and linkages to contemporary terrestrial archives.

Deep Sea Drilling Program (DSDP) Site 231 (11.89°N, 48.25°E, 2152 m water depth, DSDP Leg 24) is the closest Plio-Pleistocene marine sedimentary record to the East African Rift System. The core site is located in the central Gulf of Aden, south of the central spreading rift axis ridge, at 500–2000 km from East African volcanoes and within range of many explosive events (Fig. 1) (Pyle, 1999). Six visible tephra layers have been identified within the nannofossil ooze in DSDP Site 231 (Bunce and Fisher, 1974) and geochemically correlated to tuffs in the Turkana Basin, Kenya and Ethiopia (Sarna-Wojcicki et al., 1985; Brown et al., 1992) (Table 1) providing the basis for an interpolated age model for the core (Fig. 2). These tephra provide initial age control for the sedimentary archive of terrestrial dust and plant leaf waxes in the core, documenting variable environmental aridity and vegetation type in East Africa during the last 4 Ma (deMenocal and Bloemendal, 1995; Feakins et al., 2005). Hundreds of additional silicic

* Corresponding author. Current address: California Institute of Technology, Mail Stop 100-23, Pasadena, CA 91125, United States. Tel.: +1 626 395 1785; fax: +1 626 683 0621.
E-mail address: feakins@gps.caltech.edu (S.J. Feakins).

1464-343X/$ - see front matter © 2007 Elsevier Ltd. All rights reserved.
doi:10.1016/j.jafrearsci.2007.05.004

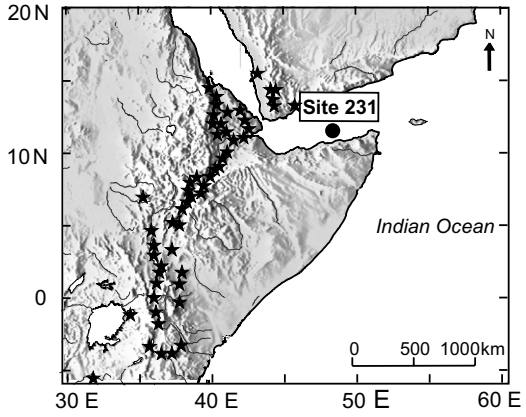

Fig. 1. Location of DSDP Site 231 in the central Gulf of Aden. Areas of known volcanic activity during the Pliocene and Pleistocene are identified with asterisks (Siebert and Simkin, 2002).

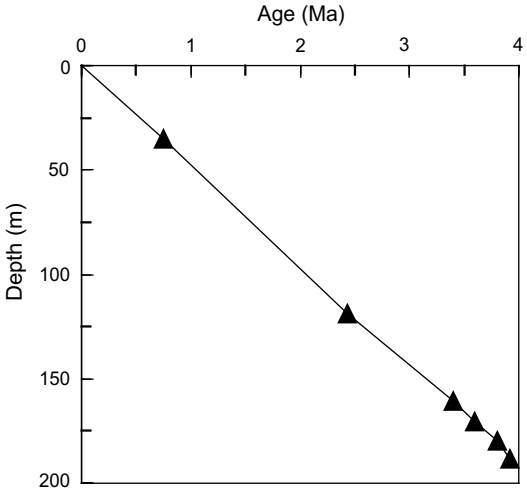

Fig. 2. Tephrostratigraphic age model for DSDP Site 231 based on linear interpolation between dated horizons (solid triangles) detailed in Table 1.

eruptions are recorded in East Africa throughout the last 4 Ma (e.g., de Heinzelin, 1983; Brown and Feibel, 1986; Harris et al., 1988; Brown et al., 1992; Feibel, 1999; Katoh et al., 2000). Since many of these Plio-Pleistocene tuffs originate from volcanoes in the Main Ethiopian Rift (Hart et al., 1992), we suspect that tephra from many additional eruptions may have reached DSDP Site 231.

Elsewhere, microscopic examination of sediments has extended regional stratigraphic correlations by detecting tephra in horizons not visible to the naked eye, notably in peat deposits in northern Britain (e.g., Turney et al., 1997) and Scandinavia (e.g., Wastegard et al., 1998). These tephra deposits have interchangeably been termed microtephra (e.g., Turney et al., 1997; Wastegard et al., 2000; Davies et al., 2001; King et al., 2001; Mackie et al., 2002; Davies et al., 2003) and cryptotephra (Chambers et al., 2004; Turney et al., 2004; Ranner et al., 2005; Gehrels et al., 2006); we use the more prevalent term, microtephra, here.

Microscopic analysis of sediments from ODP Site 721 in the northeast Indian Ocean revealed 25 discrete microtephra horizons within the Plio-Pleistocene interval (deMenocal and Brown, 1999). Geochemical correlations were established for five of the most abundant tephra horizons corresponding to the β-Tulu Bor, Lomogol, Lokochot, Wargolo and Moiti Tuffs in East Africa (deMenocal and Brown, 1999). These tephra (except for the Lokochot) appear as macroscopic horizons in DSDP Site 231 (Table 1). There is excellent potential for the identification of additional microtephra horizons in DSDP Site 231 given its proximity to the volcanoes of the East African Rift System and its flanks.

We examine DSDP Site 231 for microtephra occurrences during the last 4 Ma and seek correlations to known tuffs from the East African Rift System, based on major and minor element geochemical compositions. The resulting systematic microtephrostratigraphy offers insights into eruptive histories as well as the potential for new chronostratigraphic tie points with which to link the marine and terrestrial sedimentary records.

2. Method

We sampled 5 cm^3 of sediment by laterally scrape-sampling along 10–15 cm contiguous intervals in order to collect material continuously throughout more than 200 m sediment depth, collecting over 1050 samples. Unfortunately we were unable to sample a complete sedimentary record of the past 4 Ma given the incomplete sediment core recovery at DSDP Site 231. Core recovery during rotary

Table 1
Tephrostratigraphic age model for DSDP Site 231

Depth (m)	Age (Ma)	Tuff	Reference	Dating	Reference
35.25	0.75 ± 0.02	Silbo	B	$^{40}Ar/^{39}Ar$	McDougall and Brown (2006)
118.60	2.43 ± 0.05	Kokiselei	B	Interpolation	Brown et al. (1992)
160.80	3.40 ± 0.03	β-Tulu Bor	SW; B	$^{40}Ar/^{39}Ar$	Walter and Aronson (1993)
170.75	3.60	Lomogol	B	Interpolation	Brown et al. (1992)
179.70	3.80	Wargolo	SW; B	Interpolation	Haileab and Brown (1994) and Brown (1994)
188.35	3.92 ± 0.04	Moiti	SW; B	$^{40}Ar/^{39}Ar$	McDougall (1985)

B = Brown et al. (1992); SW = Sarna-Wojcicki et al. (1985).

drilling of DSDP Site 231 averaged 59% in the upper 4 Ma, with 66% core recovery between 1 and 4 Ma and only 39% in the upper 1 Ma (Fig. 3). Drilling disturbance of sediments was carefully noted where this would interfere with the stratigraphic record. Samples are labeled using the DSDP system, Site-Core-Section (top depth-bottom depth) e.g. 231-8-6 (30–45 cm). Each scrape sample integrates c. 2.5–3 ka as estimated by the initial tephrostratigraphic age model for the core based on published correlations for six tephra horizons (Sarna-Wojcicki et al., 1985; Brown et al., 1992) (Table 1). Discontinuous core recovery suggests considerable uncertainty in the interpolated age model between 3.4 Ma and the present.

Samples were prepared for tephra shard counts and geochemical analysis using density separation method of microtephra recovery first developed for peat cores (Pilcher and Hall, 1996; Hall and Pilcher, 2002) and later modified for mineral rich sediments (Turney, 1998; deMenocal and Brown, 1999), avoiding combustion and harsh chemical digestions that have been shown to dissolve and alter the geochemical composition of tephra shards (Blockley et al., 2005). Approximately 5 g of wet bulk sediment were treated with acetic acid to remove carbonates and with hydrogen peroxide to remove organic matter. Samples were sieved with a water jet to separate the >32 μm coarse fraction. An aliquot of the coarse fraction was mounted onto slides with coverslips and Norland optical adhesive. Care was taken to mount grains with a consistent density on the slides to make tephra concentration statistics meaningful. Tephra shards were identified by visual examination under magnification (10–40×) on a polarizing microscope. Shards were counted on a 1 cm^2 area of the slide providing a semi-quantitative measure of tephra concentration. Optically isotropic properties and shard morphology are together diagnostic of volcanic glass shards. For those samples where microtephra abundances were detected, tephra shards were concentrated from the >32 μm coarse fraction using sodium polytungstate (SPT) heavy liquid separation to remove biogenic silica (<2.2 g cm^{-3}) and heavy mineral fractions (>2.4 g cm^{-3}). Experimental extractions indicate that >80% of tephra shards are recovered from the 2.2–2.4 g cm^{-3} density fraction.

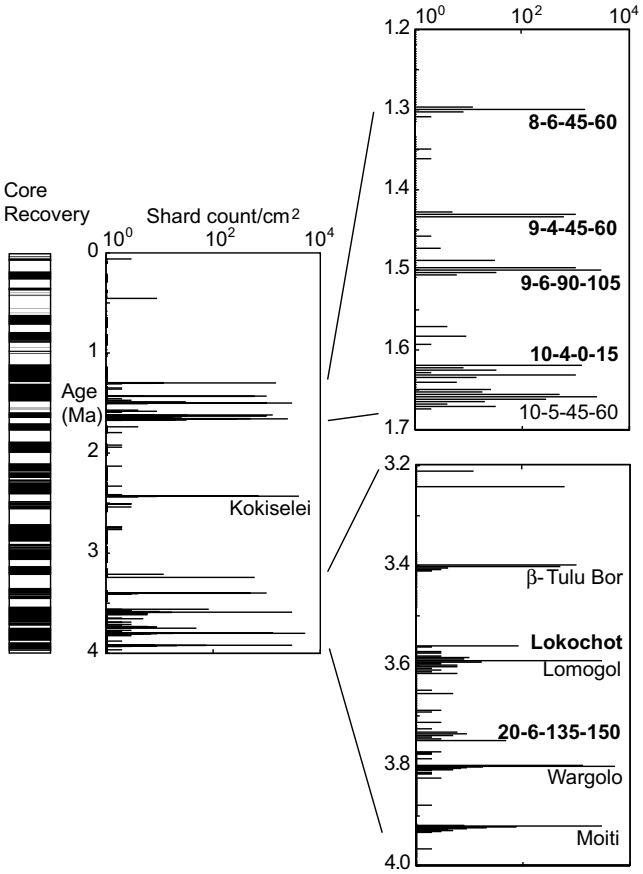

Fig. 3. Semi-quantitative shard count (number of shards/1 cm^2 of prepared slides) of volcanic glass shards in DSDP Site 231. Core recovery is shown adjacent for information. Continuous scrape-sampling provides a complete downcore sedimentary record throughout the last 4 Ma where sediments were available (solid); gaps in the sediment recovery indicate areas where no data on tephrostratigraphy are available. Previously identified macroscopic tephra layers include 10-5 (135–150 cm), the Kokiselei, β-Tulu Bor, Lomogol, Wargolo and Moiti (Sarna-Wojcicki et al., 1985; Brown et al., 1992). Newly identified microtephra horizons (highlighted in bold) include 8-6 (45–60 cm), 9-4 (45–60 cm), 9-6 (90–105 cm), 10-4 (0–15 cm), 20-1 (23–30 cm), correlated to the Lokochot Tuff in this study, and 20-6 (135–150 cm).

Tephra shards from horizons selected for geochemical analyses were mounted in epoxy, ground and polished to expose shard interiors. Individual grains were analyzed by electron microprobe for major and minor element composition using methods described in detail by Nash (1992). We limited our analysis to major and minor elements since by far the most extensive database of geochemical compositions exists for major and minor element analysis (e.g., de Heinzelin, 1983; Brown and Feibel, 1986; Harris et al., 1988; Asfaw et al., 1991; Brown et al., 1992; Haileab and Brown, 1994; Katoh et al., 2000; Nagaoka et al., 2005; WoldeGabriel et al., 2005; Brown et al., 2006). Fewer East African tephra have been characterized for trace element composition (e.g., Harris et al., 1988; Hart et al., 1992; Haileab and Brown, 1994; WoldeGabriel et al., 2005; Brown et al., 2006). All analyses were made on a Cameca SX-50 electron microprobe equipped with four wavelength-dispersive spectrometers at the University of Utah, with conditions and standards as reported in Brown et al. (2006). Elemental concentrations were converted to oxide concentrations, computing all Fe as Fe_2O_3, and then converting excess O to H_2O, following adjustment of the oxygen concentration for F and Cl by the procedure described by Nash (1992). Na_2O and K_2O are reported but are not considered in geochemical correlations given the potential for alkali exchange, especially in the terrestrial samples where depositional environments may differ strongly from site to site (Cerling et al., 1985). Measured oxides from volcanic glasses nearly always total <100% due to hydration (Steen-McIntyre, 1972). Data were not normalized to 100% given the errors that this may introduce given unknowns of

original alkali content, alkali exhange and relative Fe_2O_3 and FeO composition (Brown et al., 1992).

3. Results

Microscopic examination revealed rare tephra occurrences in the marine sediments of DSDP Site 231 (Fig. 3). Tephra were typically clear bubble wall shards and occasional bubble wall junctures. One tephra layer was characterized by vesicular bubble wall fragments. Microtephra layers were sharply defined, with abundance peaks typically restricted to one or two adjacent samples (i.e., less than 30 cm). Background shard counts of zero indicate that the marine record preserves tephra deposits with minimal reworking. Downcore shard abundance counts reveal peaks associated with individual eruptions and indicate 68 discrete tephra occurrences in addition to six macroscopically visible tephra horizons in the core.

Geochemical analyses of major element oxide concentrations were made on individual shards from microtephra horizons in DSDP Site 231. Of the 68 microtephra occurrences identified in this study we obtained sufficient shards for electron microprobe analysis for six tephra horizons. Averaged geochemical data are presented for a given tuff where the shard population is unimodal, polymodal distributions were first divided into modes principally on the basis of iron and aluminum content before averaging (Table 2). Several samples yielded polymodal shard populations which most likely indicate incorporation of tephra erupted from several sources, and mixed within the time interval of sedimentary sampling resolution (Feibel, 1999; Shane, 2000). Alternatively polymodal shard geochemistry may result from compositional gradients within the magma of an individual eruption (e.g., Hildreth, 1981). The polymodal composition of tephra highlights the need for analysis of individual grain geochemistry.

Geochemical composition and stratigraphical position were used to identify possible correlative tuffs in East Africa for tephra horizons in DSDP Site 231. All tephra with similar geochemical composition and with an estimated age of within ±0.5 Ma were included in comparisons. The closest matches are presented in this discussion and in the online supplemental data.

3.1. Tephra layer 231-8-6 (45–60 cm) (c. 1.30 Ma)

Electron microprobe analysis of glass shards extracted from 231-8-6 (45–60 cm) at a depth of 62.45 m in DSDP Site 231 reveals a broad range of geochemical compositions with a polymodal distribution (Table 2) that does not correspond to a single East African tuff. Four modal groups were assigned principally on the basis of Fe and Al composition. Fe-rich shards (M1) have a similar composition to tuff ETH90-387 (B. Haileab, pers comm. 2/23/05) from the middle Palaeolithic archaeological site at Melka Kontoure, Ethiopia (~8.7056N, 38.6064E), dating to between 1.5 and 1.0 Ma (Chavaillon et al., 1979; Clark and Kurashina, 1979; WoldeGabriel et al., 2000). 231-8-6 (45–60 cm) is estimated to date from c. 1.30 Ma based on the interpolated age model for the core; although the age model is poorly constrained in this interval (Fig. 2). Geochemical compositions for M2 and M3 do not overlap with any known African tuffs. M4 (1 shard) displays geochemical affinity to samples of the Bench Tuff, from Konso, Ethiopia (1.39 Ma) (Katoh et al., 2000), however one shard is insufficient for a reliable assessment.

The polymodal geochemical composition presumably indicates mixing of tephra from multiple eruptions. Shard counts indicate a well-defined tephra horizon within the 15 cm (~3 ka) interval integrated by scrape-sampling between 62.45 and 62.60 m, with rare shards in adjacent samples between 62.30 and 63.05 m equivalent to 15 ka (Fig. 3). Bioturbation through this 75 cm depth range could produce the polymodal shard distribution in 231-8-6 (45–60 cm) if tephra from several eruptions were mixed during this 15 ka interval. A single eruptive source of polymodal geochemical composition is less likely, since no such coeval example is known from East Africa. We are therefore unable to provide a unique correlation for this tephra layer but propose that the evidence is consistent with an age of between 1.3 and 1.4 Ma.

3.2. Tephra layer 231-9-4 (45–60 cm) (c. 1.43 Ma)

Tephra layer 231-9-4 (45–60 cm), at 68.95 m depth (c. 1.43 Ma) in DSDP Site 231, displays a unimodal clustered distribution (Table 2) with one low iron outlier excluded. Stratigraphical position suggests a potential match with the Black Pumice Tuff, identified in the Koobi Fora, Shungura and Nachukui formations in the Turkana Basin, Kenya and Ethiopia (Brown and Feibel, 1986; Haileab and Brown, 1994; Brown et al., 2006). Correlation appears unlikely based on non-overlapping distributions in MnO and MgO, however these elements are relatively mobile and so a match to the Black Pumice Tuff is not necessarily excluded.

3.3. Tephra layer 231-9-6 (90–105 cm) (c. 1.50 Ma)

The tephra layer 231-9-6 (90–105 cm) at 72.4 m depth (c. 1.50 Ma) in DSDP Site 231 has a unimodal geochemical composition defined by analyses of 70 individual shards (Table 2) with one outlier excluded. Comparison of shard geochemistry to known tuffs in the East African Rift System reveals that 231-9-6 (90–105 cm) has a unique Fe_2O_3, Al_2O_3 and MgO composition relative to East African tuffs that have been geochemically characterized.

3.4. Tephra layer 231-10-4 (0–15 cm) (c. 1.62 Ma)

Major element geochemistry for tephra layer 231-10-4 (0–15 cm) at 78.3 m depth (c. 1.62 Ma) in DSDP Site 231

Table 2
Concentration of major oxides in glass shards from trace tephra horizons in DSDP Site 231

	Average analyses of glass shards by electron microprobe (wt%)																	Total	Age (Ma)
	n	SiO_2	TiO_2	ZrO_2	Al_2O_3	Fe_2O_3	MnO	MgO	CaO	BaO	Na_2O	K_2O	F	Cl	Sum	less O	Total	H_2O		
231-8-6 (45–60 cm)																			
M1	5	72.37	0.27	0.21	10.40	4.09	0.15	0.01	0.28	0.05	2.48	3.79	0.28	0.10	94.48	0.14	94.34	8.31	102.65	1.30
1 σ	5	0.66	0.04	0.05	0.10	0.12	0.01	0.01	0.02	0.02	0.43	0.20	0.02	0.01	1.42	0.00	1.42	1.30	0.27	
M2	2	74.49	0.21	0.09	12.40	1.88	0.08	0.09	0.38	0.01	1.96	3.95	0.21	0.13	95.88	0.12	95.76	6.62	102.38	
1 σ	2	0.55	0.07	0.01	0.07	0.06	0.01	0.01	0.00	0.01	2.16	0.90	0.06	0.00	2.30	0.03	2.32	1.77	0.55	
M3	2	65.54	0.24	0.25	9.64	3.06	0.12	0.02	0.23	0.04	2.05	3.16	0.23	0.08	84.67	0.12	84.56	15.86	100.41	
1 σ	2	0.33	0.02	0.02	0.02	0.05	0.01	0.01	0.02	0.00	0.11	0.13	0.02	0.01	0.17	0.01	0.17	0.11	0.05	
M4	1	72.41	0.20	0.14	11.39	2.55	0.09	0.00	0.32	0.01	2.55	3.99	0.27	0.10	94.03	0.14	93.89	8.39	102.28	
231-9-4 (45–60 cm)																			
M1	27	70.84	0.24	0.11	13.41	2.09	0.06	0.16	0.83	0.02	2.80	4.58	0.16	0.15	95.45	0.10	95.34	6.10	101.45	1.43
1 σ	27	0.52	0.04	0.05	0.13	0.06	0.02	0.01	0.03	0.02	0.30	0.09	0.04	0.01	0.79	0.02	0.78	0.34	0.68	
231-9-6 (90–105 cm)																			
M1	70	72.70	0.22	0.12	12.21	1.70	0.10	0.10	0.39	0.03	3.22	4.23	0.19	0.13	95.35	0.11	95.24	6.98	102.22	1.50
1 σ	70	1.95	0.05	0.06	0.42	0.26	0.03	0.03	0.09	0.03	0.63	0.36	0.06	0.02	2.78	0.02	2.78	2.02	0.87	
231-10-4 (0–15 cm)																			
M1	15	69.14	0.17	0.27	11.05	2.78	0.07	0.01	0.22	0.00	2.84	3.85	0.49	0.25	91.15	0.26	90.89	10.43	101.31	1.62
1 σ	15	2.09	0.03	0.06	0.26	0.20	0.03	0.01	0.02	0.01	0.71	0.40	0.08	0.03	3.19	0.04	3.19	2.46	0.98	
231-20-1 (20–30 cm)																			
M1	14	71.78	0.18	0.24	10.46	2.83	0.08	0.03	0.18	0.00	2.30	4.27	0.28	0.13	92.76	0.15	92.61	8.87	101.48	3.56
1 σ	14	0.46	0.04	0.07	0.11	0.06	0.02	0.01	0.01	0.00	0.18	0.13	0.06	0.01	0.59	0.02	0.59	0.65	0.61	
M2	10	73.36	0.18	0.25	10.52	2.95	0.09	0.03	0.17	0.00	2.23	4.36	0.26	0.14	94.56	0.14	94.42	5.72	100.13	
1 σ	10	0.74	0.02	0.08	0.09	0.06	0.02	0.04	0.01	0.00	0.30	0.33	0.07	0.01	1.28	0.03	1.26	2.68	3.88	
M3	4	72.26	0.22	0.28	9.74	4.18	0.13	0.01	0.21	0.00	1.88	4.01	0.39	0.17	93.48	0.20	93.27	7.16	100.44	
1 σ	4	0.61	0.00	0.02	0.07	0.04	0.01	0.01	0.01	0.00	0.40	0.37	0.02	0.01	1.38	0.01	1.38	0.40	0.99	
M4	1	72.55	0.22	0.24	10.04	3.85	0.14	0.02	0.19	0.00	2.02	4.22	0.35	0.15	93.98	0.18	93.80	7.79	101.59	
231-20-6 (135–150 cm)																			
M1	1	60.50	0.13	0.24	9.57	2.34	0.10	0.00	0.12	0.00	1.64	2.71	0.33	0.12	77.82	0.17	77.65	16.48	94.14	3.75

Geochemical data for individual shards are available in the online supplemental data.

Table 3
Concentration of major oxides in glass shards from tephra horizons 231-20-1 (23–30 cm) at 168.73 m depth in DSDP Site 231 and from outcrops of the Lokochot Tuff, c. 3.58 Ma, from the Turkana Basin, Kenya and Ethiopia

Tuff	Location	Average analyses of glass shards by electron microprobe (wt%)								Reference
		N	SiO_2	TiO_2	Al_2O_3	Fe_2O_3	MnO	MgO	CaO	
231-20-1 (23–30 cm)										
M1	Gulf of Aden	14	71.78	0.18	10.46	2.83	0.08	0.03	0.18	
1 σ		14	0.46	0.04	0.11	0.06	0.02	0.01	0.01	
M2		10	73.36	0.18	10.52	2.95	0.09	0.03	0.17	
1 σ		10	0.74	0.02	0.09	0.06	0.02	0.04	0.01	
M3		4	72.26	0.22	9.74	4.18	0.13	0.01	0.21	
1 σ		4	0.61	0.00	0.07	0.04	0.01	0.01	0.01	
M4		1	72.55	0.22	10.04	3.85	0.14	0.02	0.19	
Lokochot Tuff										
K99-3949LoFe	Turkana Basin	10	73.85	0.15	10.58	2.94	0.08	na	0.16	
K99-3949HiFe	Turkana Basin	7	73.87	0.20	9.73	4.22	0.12	na	0.17	
K80-295LoFe	Turkana Basin	16	70.84	0.16	10.17	2.91	0.10	na	0.03	Brown et al. (1992)
K80-293LoFe	Turkana Basin	16	71.99	0.15	10.33	2.94	0.09	na	0.03	Brown et al. (1992)
K81-532LoFe	Turkana Basin	14	72.00	0.16	10.43	2.95	0.09	na	0.02	Brown et al. (1992)
K80-295HiFe	Turkana Basin	10	69.94	0.19	9.37	4.12	0.14	na	0.18	Brown et al. (1992)
K80-293HiFe	Turkana Basin	14	71.04	0.20	9.48	4.19	0.14	na	0.19	Brown et al. (1992)
K81-532HiFe	Turkana Basin	4	70.88	0.21	9.57	4.20	0.13	na	0.17	Brown et al. (1992)
K82-846	Turkana Basin	19	72.60	0.21	9.55	4.33	0.13	na	0.19	
K98-3705HiFe	Turkana Basin	5	74.15	0.23	10.05	4.38	0.15	na	0.19	
K00-6101	Turkana Basin	12	74.37	0.22	9.81	4.36	0.14	na	0.19	
K98-3724	Turkana Basin	2	73.27	0.21	9.92	4.40	0.14	na	0.19	
IL02-194	Turkana Basin	4	74.01	0.26	9.82	4.46	0.15	na	0.19	Gathogo and Brown (2006)
KIB02-171	Turkana Basin	4	73.53	0.24	9.52	4.00	0.12	na	0.20	Fuller pers. comm.
E04-005 M1	Turkana Basin	13	73.47	0.23	9.56	4.33	0.13	na	0.18	
UG91-1	W. Rift, Uganda	9	73.70	0.22	9.88	4.34	0.14	na	0.19	Pickford et al. (1991)
ETH86-111	Turkana Basin	9	72.68	0.21	9.60	4.30	0.12	na	0.20	Haileab (1995)
ETH86-111 M2	Turkana Basin	19	73.22	0.24	9.73	4.37	0.12	na	0.20	Haileab (1995)

are presented in Table 2. Data fall into a unimodal distribution, with two outliers excluded. Comparison to East African tuffs of comparable age and geochemical composition fails to yield a single, strong correlation. The Akait Tuff (c. 1.44 Ma) (Feibel and Brown, 1993; Brown et al., 2006) marginally overlaps in Fe_2O_3, Al_2O_3, TiO_2, CaO, MgO and MnO composition. Several other tuffs have major element geochemical compositions that overlap with the Akait Tuff including the Chari Tuff and the Nabelete Tuff (Brown et al., 2006). These tuffs all date to between 1.38 and 1.44 Ma, and indicate a common geochemical composition for eruptive events during this interval. A similar problem of geochemical correlation was identified with a macroscopic tephra horizon at 231-10-5 (45–60 cm) (Brown et al., 1992). All these tuffs, with the exception of the Akait and Nabelete Tuffs, can be distinguished based on trace element geochemistry, suggesting that additional analyses are need to adequately characterize tephra from 1.7 to 1.3 Ma in DSDP Site 231. Although we are unable to identify a single correlative tuff, geochemical similarities

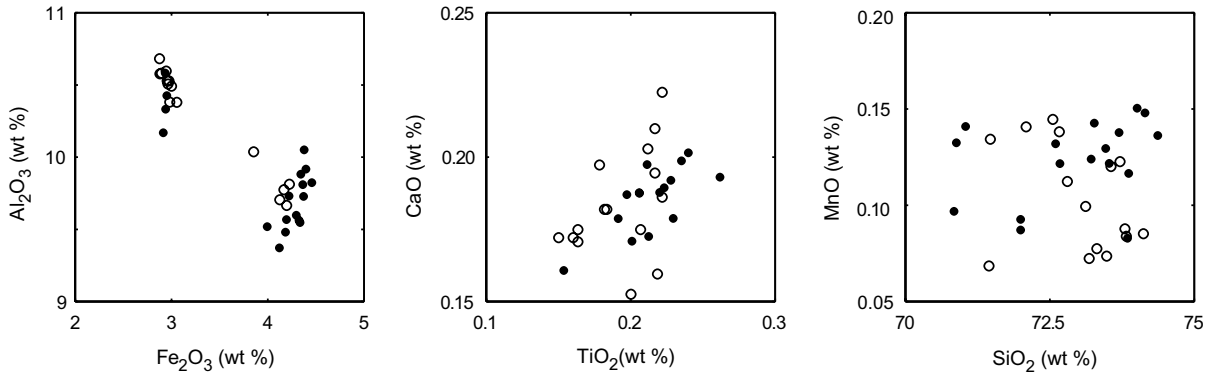

Fig. 4. Bivariate plots of Fe_2O_3 vs. Al_2O_3, TiO_2 vs. CaO, SiO_2 vs. MnO (wt%) for individual grains of tephra layer 231-20-1 (23–30 cm) (open circles). Solid circles denote average geochemical composition of tephra identified as the Lokochot tuff.

to several tuffs suggest that this tephra layer may date to c. 1.4 Ma, significantly younger than the interpolated age model estimate of 1.62 Ma.

3.5. Tephra 231-20-1 (23–30 cm) (c. 3.56 Ma) = Lokochot Tuff (3.58 Ma)

A microtephra horizon, 231-20-1 (23–30 cm), at 168.73 m depth (c. 3.56 Ma) in DSDP Site 231 indicates a bimodal composition with a strong correlation to the Lokochot Tuff (Table 3; Fig. 4). The Lokochot Tuff, so-named where it outcrops in the Koobi Fora Formation, east of Lake Turkana, has previously been correlated to tuffs at a range of sites elsewhere in the Turkana Basin, including to Tuff A in the Shungura and Usno formations, and to the Nachukui Formation by geochemical fingerprinting of glass shards (Table 3) (Brown et al., 1992; Brown, 1994). Sarna-Wojcicki et al. (1985) previously correlated a tephra horizon at 170.3 m depth (231-20-2) to the Lokochot, however this was subsequently revised and a new assignment to the Logomol was made (Brown et al., 1992). The Lokochot Tuff has also been identified in eastern Gulf of Aden at DSDP Site 232 (140.1 m depth, sample 232-16-4) (Brown et al., 1992) and Arabian Sea Site 721 (deMenocal and Brown, 1999) where it was assigned an orbitally tuned age of 3.58 ± 0.01 Ma. The Lokochot Tuff is located at the Gauss/Gilbert palaeomagnetic boundary in the Shungura Formation (Brown et al., 1978) providing a consistent age of 3.58 Ma (Hilgen et al., 1995).

3.6. Tephra layer 231-20-6 (135–150 cm) (3.75 Ma)

Major element geochemistry for tephra layer 231-20-6 (135–150 cm) at 177.35 m (c. 3.75 Ma) in DSDP Site 231 is presented in Table 2. Unfortunately, despite attempts to concentrate the rare glass shards from this sample (49 shards/cm^2), only one glass shard was successfully recovered and analyzed with the electron microprobe. The geochemical composition of this one shard, with low Al and Ca concentrations, does not display a close affinity to any known East African tuff older than 3.4 Ma.

4. Significance of the correlation to the Lokochot Tuff

Discovery of the Lokochot Tuff in DSDP Site 231 provides a tightly constrained 200 ka interval prior to the β-Tulu Bor Tuff which can now be directly compared in the marine and terrestrial sedimentary records. In the Nachukui Formation, at Lomekwi, in the Turkana Basin, Kenya the Lokochot Tuff (3.58 Ma) (Brown et al., 1978; McDougall et al., 1992) and the β-Tulu Bor Tuff (3.40 Ma) (Walter and Aronson, 1993) bracket the KNM-WT 40000 cranium, that has been attributed to *Kenyanthropus platyops* (Leakey et al., 2001). During the later part of this time interval there was a shallow lake in the Turkana Basin (Brown and Feibel, 1991; Feibel et al., 1991). Immediately below the β-Tulu Bor Tuff at Wargolo, in the Turkana Basin, we find cyclic variations in lake sedimentation. Tephrostratigraphic correlations suggest that these cycles in the Turkana Basin may correspond to precessional cyclicity in terrigenous dust concentrations and plant biomarkers in DSDP Site 231. In the marine sediments between the Lokochot and β-Tulu Bor Tuffs windblown dust concentrations vary by over 30% (deMenocal and Bloemendal, 1995) and plant wax biomarkers record a 20–30% variability in the proportion of C_4 grassland cover (Feakins et al., 2005). Thus tephrostratigraphy provides the means to link local changes in the Turkana Basin with the wider context of regional environmental change preserved in the marine record.

5. The frequency and magnitude of East African volcanism

The distribution of tephra within a distal stratigraphic sequence provides a measure of the magnitude and frequency of explosive volcanic events subject to biases in tephra eruption mode, transport and deposition. We compare the tephra flux to DSDP Site 231 as recorded by semi-quantitative microtephra abundance counts to the number of tuffs preserved in the Turkana Basin and Omo Valley (Fig. 5). The Turkana Basin and Omo Valley preserve the most complete record of eruptions in the East African Rift System with over 150 tuffs (Feibel, 1999). However, variable fluvial transport and accommodation space influences the preservation of tephra such that thickness of a tephra deposit may be unrelated to erupted volume (Feibel, 1999; Pyle, 1999). The record of microtephra abundances in DSDP Site 231 offers another perspective on tephra fluxes from the East African Rift System (Fig. 5). We find a smaller number of eruptions (68) as would be expected given the incomplete core recovery (59%) and likely variations in tephra transport trajectories and strengths.

5.1. Tephra transport considerations

Tephra from felsic, explosive eruptions are ejected high into the atmosphere and may be transported thousands of kilometers by the spreading plume. Widespread tephra from felsic volcanism, associated with Afro-Arabian continental rifting, have been identified up to 2700 km from source (deMenocal and Brown, 1999; Peate et al., 2003). The flux of tephra to distal sites is determined by the erupted volume, column height achieved and the prevailing wind strength (e.g., Shane, 2000). Wind direction and strengths throughout the troposphere and stratosphere may affect tephra dispersal since explosive eruptions with erupted volumes of greater than 2 km^3 could be sufficiently large to be transported into the stratosphere (Simkin and Siebert, 1994). For reference, the macroscopic Plio-Pleistocene tephra deposits in DSDP Site 231 are estimated to represent eruptions of greater than 40 km^3 of magma, since they have been correlated over 1500–2000 km at

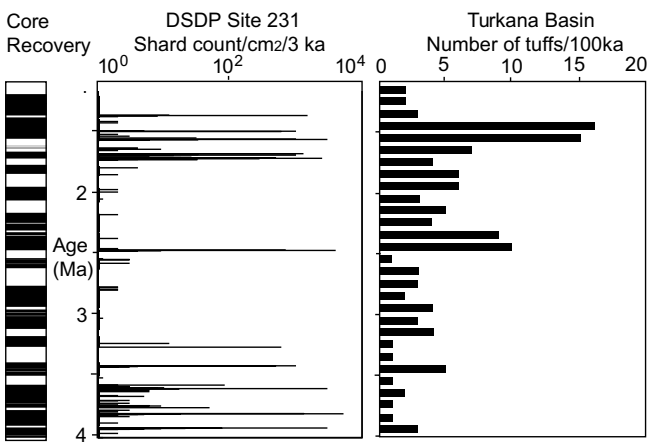

Fig. 5. Comparison of the shard count in DSDP Site 231 and the number of tuffs discovered in the Turkana Basin in 100 ka intervals between 4 and 1 Ma (after Feibel, 1999). The number of tuffs in the Turkana Basin provides information on eruptive frequency. The shard count in DSDP Site 231 provides a semi-quantitative measure of the magnitude of volcanic activity. Neither tephrostratigraphic records is expected to provide a complete record of East African explosive volcanism over the past 4 Ma given the possibility that tephra from an eruption may not reach a given location, from lack of suitable depositional environment (Turkana Basin) or from gaps in sediment recovery (DSDP drilling). Core recovery is shown for DSDP Site 231 (solid bars). Together the records indicate three pulses of volcanism, particularly between 4.0 and 3.4 Ma, 2.7 and 2.5 Ma and 2 and 1.3 Ma.

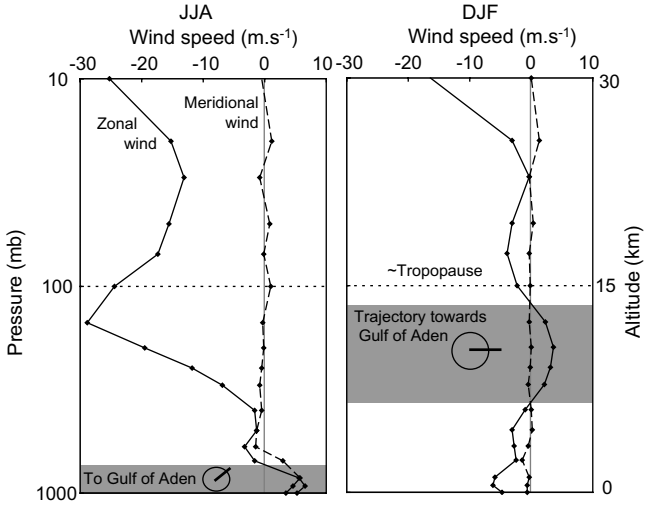

Fig. 6. Velocity profile vertically through the atmosphere for mean zonal and meridional winds over the Horn of Africa during the contrasting summer and winter monsoon months of (a) June, July and August and (b) December, January and February. Wind velocities were obtained from the NOAA NCEP CDAS-1 monthly pressure level climatology calculated from a dataset spanning January 1949–November 1961 averaged over the area 38.75–51.25°E, 1.25–16.25°N (Kalnay et al., 1996). The approximate altitude and the height of the tropopause are given for reference with respect to the vertical pressure. Positive (negative) values indicate westerly (easterly) flow for the zonal component and northerly (southerly) flow for the meridional component. Wind directions towards the Gulf of Aden are highlighted (shaded regions, wind rose). Favorable wind trajectories for tephra transport from eruptions in East Africa towards the Gulf of Aden vary with the seasonal changes in atmospheric circulation.

thicknesses of over 10 cm (Pyle, 1999). These large volume Plio-Pleistocene eruptions would likely have supplied tephra throughout the troposphere and stratosphere, whereas smaller volume or less explosive eruptions may have been confined to lower altitudes.

Surface winds during the summer monsoon have been observed to transport dust from East Africa to the Gulf of Aden (Prospero et al., 2002). In the modern atmosphere, maximum southwest monsoon wind speeds during June, July and August average over 5 m s^{-1} in the lower troposphere (Kalnay et al., 1996) (Fig. 6). These southwesterly winds could transport tephra in low altitude eruption plumes towards the Gulf of Aden (deMenocal and Brown, 1999). During the same season, in the upper troposphere and stratosphere, strong easterly flow would inhibit tephra fluxes to the Gulf of Aden, particularly for eruptive plumes reaching elevations of >7 km. For eruptions during the summer monsoon circulation, a measurable tephra flux may still reach the Gulf of Aden even if only a small fraction of the erupted material is transported in the lower atmosphere, however the magnitude of the tephra flux reaching the Gulf of Aden may be severely attenuated for high altitude eruption plumes carried by the easterly upper air flow.

In the winter months the wind direction reverses to an easterly direction in the lower troposphere (Fig. 6). Although easterlies in the stratosphere weaken relative to the summer months, flow remains in an easterly direction, inhibiting tephra fluxes to the Gulf of Aden. Only for tephra in the upper troposphere, c. 7–12 km elevation, would westerly winds favor transport from East Africa to the Gulf of Aden. Since many explosive eruptions reach this altitude, this limited region of favorable transport to the Gulf of Aden may be sufficient to transport a fraction of the tephra plume from explosive eruptions.

Clearly the tephra flux to the Gulf of Aden must be significantly influenced by the height of the eruptive column and seasonal wind reversals (Fig. 6). In addition past variations in seasonal wind speeds and circulation patterns may have influenced tephra transport, such as the southward shift of the westerlies during glacial times (Clemens and Prell, 1990). However without seasonal resolution of the timing of eruptions, there is little scope to assess the impact of seasonally reversing patterns of atmospheric circulation on tephra dispersal.

Transport within the ocean may also influence the tephrostratigraphic record. Density instabilities have been shown to increase tephra settling velocities in the ocean, reducing residence time and the potential for lateral advection, but introducing the possibility of sedimentary patterns associated with density currents (Carey, 1997; Manville and Wilson, 2003). However, observation of tephra deposition following the 1991 Mount Pinatubo eruption demonstrated that the sedimentary signature of tephra in deep sea sediments largely preserved the atmospheric transport direction and fallout pattern (Wiesner et al., 2004). Considering atmospheric and oceanic transport it is not surprising that a significant proportion of East

African eruptions are recorded with microtephra abundances in DSDP Site 231, however abundances may be only weakly related to eruption magnitude.

6. The Plio-Pleistocene tephrostratigraphic record

The microscopic tephrostratigraphy of DSDP Site 231 confirms the evidence for three pulses of three pulses of explosive volcanic activity from 4.0 to 3.2 Ma, c. 2.5 Ma and 1.7 to 1.3 Ma described in the Turkana Basin (Haileab and Brown, 1994; Feibel, 1999). The first peak in volcanic activity is seen with widespread, large volume tephra deposits between 4.0 to 3.2 Ma in both the Turkana Basin and DSDP Site 231. Tuffs of this age are commonly very voluminous where they outcrop in the Turkana Basin (e.g., the β-Tulu Bor Tuff) is typically c. 5 m thick (Brown and Feibel, 1986). Four of these widespread tephra have previously been correlated to horizons in the Gulf of Aden, (Sarna-Wojcicki et al., 1985; Brown et al., 1992) where the β-Tulu Bor tuff forms a visible horizon 25 cm thick with microscopic tephra concentrations throughout 60 cm of sediment (Fig. 3). In this study we add an additional correlation of a microtephra horizon at 168.73 m depth to the Lokochot Tuff (c. 3.58 Ma). While this tuff is documented with a thickness of 2 m in the Turkana Basin (Brown and Feibel, 1986), it is only microscopically detected in DSDP Site 231 within 20 cm of sediment, indicating less favorable eruptive or atmospheric conditions for tephra dispersal relative to the other widespread Pliocene eruptions.

A second peak of volcanic activity is recorded between 2.75 and 2.25 Ma in the Turkana Basin. A single macroscopic tuff, correlative to the Kokiselei Tuff in the Turkana Basin, is visible in this interval (Brown et al., 1992) along with several microtephra horizons reported here (Fig. 3). Poor sediment core recovery hampers our interpretation of explosive volcanism during this interval given the large gaps of 6.5 m (between c. 2.74 and 2.59 Ma) and 3 m (from c. 2.44 to 2.50 Ma).

The third interval of frequent volcanic activity from 1.7 to 1.3 Ma was characterized by smaller volume, or more weakly transported tephra deposits, most of which were only present in trace quantities in DSDP Site 231 (Fig. 5). In the Turkana Basin the highest Plio-Pleistocene tephra frequency is recorded between 1.75 and 1.25 Ma (equivalent to one eruption every 3 ka), with many additional tephra deposited throughout the interval 2.0–1.25 Ma (Feibel, 1999; McDougall and Brown, 2006). A similar pattern is documented near Konso, Ethiopia, where rifting and volcanic activity intensified in the early Pleistocene (between 1.9 and 1.4 Ma) in the southern Main Ethiopian Rift (Katoh et al., 2000; Nagaoka et al., 2005; WoldeGabriel et al., 2005). The Konso tephrostratigraphy reveals an increasing frequency of tephra between 1.91 and 1.33 Ma, recording a peak eruptive frequency of one eruption every 10 ka between 1.41 and 1.33 Ma (WoldeGabriel et al., 2005). In the marine record this early Pleistocene pulse of volcanic activity yields 18 microtephra horizons from widespread eruptions (Fig. 3). Additional widespread tephra may have been deposited in several gaps in sediment core recovery between 2.0 and 1.5 Ma. Only one eruption during this interval was of sufficiently large volume or effectively transported to deposit a macroscopically visible ash layer in the central Gulf of Aden (Brown et al., 1992).

At this time we are unable to geochemically correlate the microtephra deposits in DSDP Site 231 estimated to between 1.7 and 1.3 Ma (Table 2) with tephra from the East African Rift System. In the Turkana Basin too, many more tephra have been identified than can be regionally correlated or dated. Between 1.7 and 1.4 Ma, 65 tephra have been identified in the Turkana Basin (McDougall and Brown, 2006). Fewer than a third of these tephra have been correlated (Brown et al., 2006). The high frequency and small volume of eruptive events in this interval may explain why individual events cannot easily be geochemically characterized and differentiated: small, frequent eruptions may sample geochemically similar magma sources (Shane, 2000). Furthermore, we may not yet have a complete database of geochemical characteristics of all the eruptions in this interval. For example, remote sensing has documented extensive felsic deposits in the Nabro Volcanic Range, in the northern Afar region of Ethiopia, that have not yet been adequately sampled for geochemical composition (Wiart and Oppenheimer, 2005). Given that the adjacent Danakil Depression is an important source of dust to the Gulf of Aden (Prospero et al., 2002) it seems likely that tephra from this region would also be well represented in the marine sediments of the Gulf of Aden. Although we are presently unable to locate correlative tuffs for all of the microtephra layers identified (68) and geochemically characterized (6), the many microtephra horizons discovered in DSDP Site 231 may in the future yield age control once correlations to deposits in the East African Rift System can be established.

7. Conclusions

Tephra provide the primary means of dating and correlating disparate sedimentary archives, representing time-equivalent marker horizons independent of dating uncertainties. Microscopic tephrostratigraphy offers the means to identify many more tephra layers than are present in sufficient abundance to be visible to the naked eye. In a microscopic examination of DSDP Site 231 we identify 68 additional microtephra horizons during the last 4 Ma, an order of magnitude more tephra layers than visible to the naked eye alone.

Thickest tephra accumulations between 4.0 and 3.2 Ma indicate a pulse of widespread, large volume volcanic eruptions. Five macroscopic tephra horizons have already been correlated to East African tephra. We add an additional correlation for a microtephra horizon to the Lokochot Tuff (c. 3.58 Ma) tightly constraining mid Pliocene correlations between the fossil record of the Turkana Basin (e.g., Leakey et al., 2001) and the record of paleoclimate variability

in the marine core (deMenocal and Bloemendal, 1995; Feakins et al., 2005).

Microtephra in DSDP Site 231 offer a new perspective on the early Pleistocene pulse of volcanic activity also seen in Ethiopia and Kenya (Feibel, 1999; Katoh et al., 2000; WoldeGabriel et al., 2005). We know that high frequency eruptions between 1.7 and 1.3 Ma were less widespread than the eruptions of the early Pliocene based on their abundance in DSDP Site 231. Geochemical correlations of these early Pleistocene tephra has met with less success than the mid Pliocene large volume eruptions due to various issues including insufficient shard recovery, polymodal shard populations (perhaps resulting from bioturbation of closely spaced eruptions), absence of correlative tuffs (perhaps originating from as yet unsampled regions of Ethiopia) and non-unique major and minor element composition, which could potentially be solved with trace element and isotopic analyses. To some extent these difficulties may be inherent to geochemically differentiating and correlating high frequency, small volume eruptions.

Acknowledgements

Funding was provided by the U.S. National Science Foundation HOMINID Grant 0218511 and a NOAA/UCAR Global and Climate Change Postdoctoral Fellowship to SF. We are grateful for helpful discussions and comments provided by Craig Feibel, Bereket Haileab, Jay Quade, Allegra Legrande and several anonymous reviewers. Laboratory assistance was provided by Linda Baker, Pat Malone and Quintin Sahratian. This is Lamont-Doherty Earth Observatory Publication Number 7024.

Appendix A. Supplementary data

Supplementary data associated with this article can be found, in the online version, at doi:10.1016/j.jafrearsci.2007.05.004.

References

Asfaw, B., Beyene, Y., Semaw, S., Suwa, G., White, F., WoldeGabriel, G., 1991. Fejej: a new paleoanthropological research area in Ethiopia. Journal of Human Evolution 21, 137–143.

Blockley, S.P.E., Pyne-O'Donnell, S.D.F., Lowe, J.J., Matthews, I.P., Stone, A., Pollard, A.M., Turney, C.S.M., Molyneux, E.G., 2005. A new and less destructive laboratory procedure for the physical separation of distal glass tephra shards from sediments. Quaternary Science Reviews 24 (16–17), 1952–1960.

Brown, F.H., 1994. Development of Pliocene and Pleistocene chronology of the Turkana Basin, East Africa, and its relation to other sites. In: Corruccini, R., Cioilion, R. (Eds.), Integrative Paths to the Past. Prentice Hall, Englewood Cliffs, NJ, pp. 285–312.

Brown, F., Feibel, C.S., 1986. Revision of lithostratigraphic nomenclature in the Koobi Fora region, Kenya. Journal of the Geological Society, London 143, 297–310.

Brown, F.H., Feibel, C.S., 1991. Stratigraphy, depositional environments and palaeogeography of the Koobi Fora Formation. In: Harris, J.M. (Ed.), The Fossil Ungulates: Geology, Fossil Artiodactyls, and Palaeoenvironments, vol. 3. Clarendon Press, Oxford, pp. 1–30.

Brown, F., Shuey, R., Croes, M., 1978. Magnetostratigraphy of the Shungura and Usno Formations southwestern Ethiopia: new data and comprehensive reanalysis. Geophysical Journal of the Royal Astronomical Society 54, 519–538.

Brown, F.H., Sarna-Wojcicki, A.M., Meyer, C.E., Haileab, B., 1992. Correlation of Pliocene and Pleistocene tephra layers between the Turkana Basin of East Africa and the Gulf of Aden. Quaternary International 13–14, 55–67.

Brown, F.H., Haileab, B., McDougall, I., 2006. Sequence of tuffs between the KBS Tuff and the Chari Tuff in the Turkana Basin, Kenya and Ethiopia. Journal of the Geological Society 163, 185–204.

Bunce, E., Fisher, R., 1974. Introduction. In: Fisher, R., Bunce, E. (Eds.), Initial Proceedings of the Deep Sea Drilling Program, vol. 24. U.S. Government Printing Office, Washington, pp. 3–16.

Carey, S., 1997. Influence of convective sedimentation on the formation of widespread tephra fall layers in the deep sea. Geology 25 (9), 839–842.

Cerling, T.E., Brown, F.H., Bowman, J.R., 1985. Low-temperature alteration of volcanic glass – hydration, Na, K, 18O and Ar mobility. Chemical Geology 52, 281–293.

Chambers, F.M., Daniell, J.R.G., Hunt, J.B., Molloy, K., O'Connell, M., 2004. Tephrostratigraphy of An Loch Mor, Inis Oirr, western Ireland: implications for Holocene tephrochronology in the northeastern Atlantic region. Holocene 14 (5), 703–720.

Chavaillon, J., Chavaillon, N., Hours, F., Piperno, M., 1979. From the Oldowan to the Middle Stone Age at Melka-Kunture (Ethiopia). Understanding Cultural Changes. Quaternaria 21, 87–114.

Clark, J.D., Kurashina, H., 1979. Hominid occupation of the East-Central Highlands of Ethiopia in the Plio-Pleistocene. Nature 282, 33–39.

Clark, J.D., de Heinzelin, J., Schick, K., Hart, W., White, T., WoldeGabriel, G., Walter, R.C., Suwa, G., Asfaw, B., Vrba, E., Selassie, Y., 1994. African *Homo erectus*: Old radiometric ages and Young Oldowan Assemblages in the Middle Awash Valley, Ethiopia. Science 264, 1907–1910.

Clemens, S.C., Prell, W.L., 1990. Late Pleistocene variability of Arabian Sea summer monsoon winds and continental aridity: Eolian records from the lithogenic component of deep-sea sediments. Paleoceanography 5, 109–145.

Davies, S.M., Turney, C.S.M., Lowe, J.J., 2001. Identification and significance of a visible, basalt-rich Vedde Ash layer in a Late-glacial sequence on the Isle of Skye, Inner Hebrides, Scotland. Journal of Quaternary Science 16 (2), 99–104.

Davies, S.M., Wastegard, S., Wohlfarth, B., 2003. Extending the limits of the Borrobol Tephra to Scandinavia and detection of new early Holocene tephras. Quaternary Research 59 (3), 345–352.

de Heinzelin, J., 1983. The Omo group, 85, Koninklijk Museum voor Midden-Africa, Tervuren, Geologische Wetenschappen.

deMenocal, P., Bloemendal, J., 1995. Plio-Pleistocene climatic variability in subtropical Africa and the paleoenvironment of hominid evolution: a combined data-model approach. In: Vrba, E., Denton, G., Partridge, T., Burckle, L. (Eds.), Paleoclimate and Evolution. Yale University Press, New Haven, pp. 262–288.

deMenocal, P.B., Brown, F.H., 1999. Pliocene tephra correlations between East African hominid localities, the Gulf of Aden, and the Arabian Sea. In: Agusti, J., Rook, L., Andrews, P. (Eds.), Hominid Evolution and Climatic Change in Europe, vol. 1. Cambridge University Press, pp. 23–54.

Feakins, S., deMenocal, P., Eglinton, T., 2005. Biomarker records of Late Neogene changes in East African vegetation. Geology 33, 977–980.

Feibel, C.S., 1999. Tephrostratigraphy and geological context in Paleoanthropology. Evolutionary Anthropology 8, 87–100.

Feibel, C.S., Brown, F., 1993. Microstratigraphy and paleoenvironments. In: Walker, A., Leakey, R. (Eds.), The Nariokotome Homo erectus Skeleton. Harvard University Press, Cambridge, pp. 21–39.

Feibel, C.S., Harris, J.M., Brown, F.H., 1991. Paleoenvironmental context for the late Neogene of the Turkana Basin. In: Harris, J.M. (Ed.), The Fossilungulates: Geology, Fossil Artiodactyls, and Palaeoenvironments, vol. 3. Clarendon Press, Oxford, pp. 321–370.

Gathogo, P.N., Brown, F., 2006. Stratigraphy of the Koobi Fora Formation (Pliocene and Pleistocene) in the Ileret region of northern Kenya. Journal of African Earth Sciences 45, 369–390.

Gehrels, M., Lowe, D.J., Hazell, Z., Newnham, R., 2006. A continuous 5300-yr Holocene cryptotephrostratigraphic record from northern New Zealand and implications for tephrochronology and volcanic-hazard assessment. The Holocene 16, 173–187.

Haileab, B., Brown, F.H., 1994. Tephra correlation between the Gadeb prehistoric site and the Turkana Basin. Journal of Human Evolution 26, 167–173.

Haileab, B., 1995. Geochronology, Geochemistry and Tephrostratigraphy of the Turkana Basin, Southwestern Ethiopia, Northern Kenya, PhD thesis, University of Utah. pp. 369.

Hall, V.A., Pilcher, J.R., 2002. Late-Quaternary Icelandic tephras in Ireland and Great Britain: detection, characterization and usefulness. Holocene 12 (2), 223–230.

Harris, J.M., Brown, F.H., Leakey, M.G., 1988. Stratigraphy and Paleontology of Pliocene and Pleistocene Localities West of Lake Turkana, Kenya. National History Museum of Los Angeles County, Los Angeles.

Hart, W.K., Walter, R.C., WoldeGabriel, G., 1992. Tephra sources and correlations in Ethiopia: application of elemental and neodymium isotope data. Quaternary International 13–14, 77–86.

Hildreth, W., 1981. Gradients in silicic magma chambers: implications for litheospheric magmatism. Journal of Geophysical Research 86, 10153–10192.

Hilgen, F., Krijgsman, W., Langereis, C., Lourens, L.J., Santarelli, A., Zachariasse, W.J., 1995. Extending the astronomical (polarity) time scale into the Miocene. Earth and Planetary Science Letters 136, 495–510.

Kalnay, E., Kanamitsu, M., Kistler, R., Collins, W., Deaven, D., Gandin, L., Iredell, M., Saha, S., White, G., Woolen, J., Zhu, Y., Chelliah, M., Ebisuzaki, W., Higgins, W., Janowiak, J., Mo, K., Ropelewski, C., Wang, J., Leetma, A., Reynolds, R., Jenne, R., Joseph, D., 1996. The NCEP/NCAR 40 year reanalysis project. Bulletin of the American Meteorological Society 77, 437–471. doi:10.1175/1520-0477 077<0437:TNYRP>2.0.CO;2.

Katoh, S., Nagaoka, S., WoldeGabriel, G., Renne, P., Snow, M., Beyene, Y., Suwa, G., 2000. Chronostratigraphy and correlation of the Plio-Pleistocene tephra layers of the Konso Formation, southern Main Ethiopian Rift, Ethiopia. Quaternary Science Reviews 19, 1305–1317.

King, M., Busacca, A.J., Foit, F.F., Kemp, R.A., 2001. Identification of disseminated Trego Hot Springs tephra in the Palouse, Washington State. Quaternary Research 56 (2), 165–169.

Leakey, M.G., Spoor, F., Brown, F.H., Gathogo, P.N., Klarie, C., Leakey, L.N., McDougall, I., 2001. New hominin genus from eastern Africa shows diverse middle Pliocene lineages. Nature 410, 433–440.

Mackie, E.A.V., Davies, S.M., Turney, C.S.M., Dobbyn, K., Lowe, J.J., Hill, P.G., 2002. The use of magnetic separation techniques to detect basaltic microtephra in last glacial–interglacial transition (LGIT; 15–10 ka cal. BP) sediment sequences in Scotland. Scottish Journal of Geology 38, 21–30.

Manville, V., Wilson, C., 2003. Vertical density currents: a review of their potential role in the deposition and interpretation of deep-sea ash layers. Journal of the Geological Society, London 161, 947–958.

McDougall, I., 1985. 40Ar/39Ar dating of the hominid bearing Plio-Pleistocene sequence at Koobi-Fora, Lake Turkana, northern Kenya. Bulletin of the Geological Society of America 96, 159–175.

McDougall, I., Brown, F., 2006. Precise $^{40}Ar/^{39}Ar$ geochronology for the upper Koobi Fora Formation, Turkana Basin, northern Kenya. Journal of the Geological Society 163, 205–220.

McDougall, I., Brown, F.H., Cerling, T.E., Hillhouse, J.W., 1992. A reappraisal of the geomagnetic polarity time scale to 4 Ma using data from the Turkana Basin, East-Africa. Geophysical Research Letters 19 (23), 2349–2352.

Nagaoka, S., Katoh, S., WoldeGabriel, G., Sato, H., Nakaya, H., Beyene, Y., Suwa, G., 2005. Lithostratigraphy and sedimentary environments of the hominid-bearing Pliocene–Pleistocene Konso formation in the southern Main Ethiopian Rift, Ethiopia. Palaeogeography Palaeoclimatology Palaeoecology 216 (3–4), 333–357.

Nash, W., 1992. Analysis of oxygen with the electron microprobe: applications to hydrated glass and minerals. American Mineralogist 77, 453–457.

Peate, I.U., Baker, J.A., Kent, A.J.R., Al-Kadasi, M., Al-Subbary, A., Ayalew, D., Menzies, M., 2003. Correlation of Indian Ocean tephra to individual Oligocene silicic eruptions from Afro-Arabian flood volcanism. Earth and Planetary Science Letters 211 (3–4), 311–327.

Pickford, M., Senut, B., Poupeau, G., Brown, F., Haileab, B., 1991. Correlation of tephra layers from the Western Rift Valley (Uganda) to the Turkana Basin (Ethiopia/Kenya) and the Gulf of Aden. Stratigraphy 313, 223–229.

Pilcher, J.R., Hall, V.A., 1996. Tephrochronological studies in northern England. Holocene 6 (1), 100–105.

Prospero, J., Ginoux, P., Torres, O., Nicholson, S., Gill, T., 2002. Environmental characterization of global sources of atmospheric soil dust intensified with the Nimbus 7 Total Ozone Mapping Spectrometer (TOMS) absorbing aerosol product. Reviews of Geophysics, 40. doi:10.1029/2000RG00009.

Pyle, D., 1999. Widely dispersed Quaternary tephra in Africa. Global and Planetary Change 21, 95–112.

Ranner, P.H., Allen, J.R.M., Huntley, B., 2005. A new early Holocene cryptotephra from northwest Scotland. Journal of Quaternary Science 20 (3), 201–208.

Sarna-Wojcicki, A.M., Meyer, C.E., Roth, P.H., Brown, F.H., 1985. Ages of tuff beds at East African early hominid sites and sediments in the Gulf of Aden. Nature 313, 306–308.

Shane, P., 2000. Tephrochronology: a New Zealand case study. Earth and Planetary Science Letters 49, 223–259.

Siebert, L., Simkin, T., 2002. Volcanoes of the World: an Illustrated Catalog of Holocene Volcanoes and their Eruptions. Smithsonian Institution.

Simkin, T., Siebert, L., 1994. Volcanoes of the World. Geoscience Press, Tucson.

Steen-McIntyre, V., 1972. A manual for tephrochronology. Idaho Springs, Colorado.

Turney, C.S.M., 1998. Extraction of rhyolitic component of Vedde microtephra from minerogenic lake sediments. Journal of Paleolimnology 19 (2), 199–206.

Turney, C.S.M., Harkness, D.D., Lowe, J.J., 1997. The use of microtephra horizons to correlate Late-glacial lake sediment successions in Scotland. Journal of Quaternary Science 12 (6), 525–531.

Turney, C.S.M., Lowe, J.J., Davies, S.M., Hall, V., Lowe, D.J., Wastegard, S., Hoek, W.Z., Alloway, B., 2004. Tephrochronology of Last Termination Sequences in Europe: a protocol for improved analytical precision and robust correlation procedures (a joint SCOTAV-INTIMATE proposal). Journal of Quaternary Science 19 (2), 111–120.

Walter, R.C., Aronson, J., 1993. Age and source of the Sidi Hakoma Tuff, Hadar Formation, Ethiopia. Journal of Human Evolution 25, 229–240.

Wastegard, S., Bjorck, S., Possnert, G., Wohlfarth, B., 1998. Evidence for the occurrence of Vedde ash in Sweden: radiocarbon and calendar age estimates. Journal of Quaternary Science 13 (3), 271–274.

Wastegard, S., Wohlfarth, B., Subetto, D.A., Sapelko, T.V., 2000. Extending the known distribution of the Younger Dryas Vedde Ash into northwestern Russia. Journal of Quaternary Science 15 (6), 581–586.

Wiart, P., Oppenheimer, C., 2005. Large magnitude silicic volcanism in north Afar: The Nabro Volcanic Range and Ma'alalta volcano. Bulletin of Volcanology 67 (2), 99–115.

Wiesner, M.G., Wetzel, A., Catane, S.G., Listanco, E.L., Mirabueno, H.T., 2004. Grain size, areal thickness distribution and controls on sedimentation of the 1991 Mount Pinatubo tephra layer in the South China Sea. Bulletin of Volcanology 66 (3), 226–242.

WoldeGabriel, G., Heiken, G., White, T., Asfaw, B., Hart, W., Renne, P.R., 2000. Volcanism, tectonism, sedimentation and the paleoanthropological record in the Ethiopian Rift System. In: McCoy, F.W., Heiken, G., (Eds.), Volcanic Hazards and Disasters in Human Antiquity Geological Society of America Special Paper 345, Boulder, CO.

WoldeGabriel, G., Hart, W.K., Katoh, S., Beyene, Y., Suwa, G., 2005. Correlation of Plio-Pleistocene Tephra in Ethiopian and Kenyan rift basins: Temporal calibration of geological features and hominid fossil records. Journal of Volcanology and Geothermal Research 147 (1–2), 81–108.